

Smart-Optical Detector Array in CMOS for Absorbance Measurement of Physiological Fluids

A. V. Fernandes, C. Pinheiro, J. G. Rocha, G. Minas
Dept. of Industrial Electronics
University of Minho

Campus de Azurém, 4800-058 Guimaraes, Portugal

Email: afernandes@dei.uminho.pt, cpinheiro@dei.uminho.pt, gerardo@dei.uminho.pt, gminas@dei.uminho.pt

Abstract— This paper describes a smart-optical detector array for application in microchip size analytical laboratories for physiological fluids measurement by absorbance. For this purpose, an array of optical detectors with analog-to-digital conversion is designed and fabricated in a standard CMOS process. Its application is in the low-cost measurement of physiological fluids by optical absorption, e.g., a microplate cuvette array containing the physiological fluids in analysis is placed on top of the optical detector array that quantify the light absorbed by those fluids. The on-chip analog-to-digital conversion is performed using a one-bit first-order sigma-delta converter for each optical detector. The output signal of the device is a bit stream containing information about the absorbed light, which allows simple computer interfacing. This scheme of having simultaneous measurement of the light absorbed by the fluids avoids the errors that can be introduced due to the light fluctuations and performs on-chip calibration during each measurement allowing a non-calibrated light source.

I. INTRODUCTION

The healthcare system is under pressure to provide better service at a lower price. Thus, more cost-efficient practices are needed and one of the places to improve the efficiency is at the physician's office. When the physician is confronted with an ill patient he will start looking for symptoms. However, when these symptoms lead to a wrong diagnosis, there is a problem for the physician, the patient and the society. A wrong diagnosis can lead to a wrong treatment that ultimately brings further harm to the patient and increases society expenses. The best way of increasing the diagnosis quality is to give the physician more accurate information about the state of the patient. Presently, this information is often based on the measurement of biochemical parameters in physiological fluids, such as albumin concentration in blood. Most diseases leave a molecular fingerprint in those fluids and by measuring that fingerprint in the right way, the precision of the diagnostic can be increased. Therefore, the biochemical analysis of patient's physiological fluids is a good start.

Usually, this kind of analyses is carried out in clinical laboratories, so, or the samples need to be sent to the laboratory, or the patient needs to move there for collecting the samples, and the results become available after several hours, sometimes days. As a consequence a reliable diagnosis cannot be performed within the consultation time. Mistakes in the

logistics, such as lost samples and mislabeling, may further delay the diagnosis [1]. Therefore, there is a large demand in the healthcare system to develop analytical laboratories of a microchip size for on-line measurements with low-samples volumes and at any location. The small scale allows the integration of various processes in a single chip analogous to the ones used in integrated microelectronic circuitry [2]. The advantages associated with shrinking clinical analysis systems include: small sample volume, high-degree of system integration, automation of measurement, short response time, improved analytical performance and laboratory safety and reduced cost [3]. Such microlaboratories would significantly enhance the quality of a diagnostic, by offering immediate measurement of several clinically relevant parameters that can be used to assess patient's health.

II. ABSORBANCE MEASUREMENTS IN PHYSIOLOGICAL FLUIDS

The most commonly used analytical technique for routine analysis of biochemical substances that are present in patient's physiological fluids is the colorimetric detection by optical absorption. It allows the selective detection and the concentration measurement of those biochemical substances [4]. The measurement is based on colorimetric detection by the optical absorption in a part of the visible spectrum defined by the mixture of a proper reagent with the biochemical substance present in the fluid sample. These mixtures have an absorption maximum at a specific wavelength. The absorbance value at this wavelength is directly proportional to the concentration of the biochemical substance in the samples. These measurements require further explanation. The sample is excited by a light source of intensity, I_0 , and the light intensity, I , transmitted through the sample is measured. The ratio of the two previous quantities is denominated as the absorbance, A , and is linked to the concentration of the biochemical substance according to the Lambert-Beer's law [5]:

$$A = -\log(I/I_0) = \alpha c d \quad (1)$$

where d is the pathlength, c is the concentration of the biochemical substance in the sample and α its corresponding molar absorption coefficient.

III. DEVICE STRUCTURE AND OPERATION

The complete device intended to solve the reported difficulties, e.g., it is developed for being used by the physician at his office allowing a first diagnostic within the consultation time. Moreover, due to its small-size, it uses only $0.8 \mu\text{l}$ of samples and reagents (the state-of-the-art equipment used in clinical laboratories uses 1 ml).

Usually, on-chip microlaboratories are composed by two dies: the fluid and the detection. In the reported device, the fluid die is a microplate cuvette array that contains the fluids into analysis (Fig. 1). It comprises twelve cuvettes allowing the simultaneous analysis of four biochemical parameters in physiological fluids. The analysis of each biochemical parameter requires the simultaneous measurement of the optical absorption of three fluids. So, each line of the cuvettes array, which corresponds to the analysis of one biochemical parameter, contains three cuvettes: the first is needed to obtain the baseline reference and to compensate light fluctuations; the second allows the analysis of the mixed solution; and the third is needed to calibrate the biochemical parameter concentration (it contains a standard with a well-known concentration of the biochemical parameter that is being analyzed). This scheme of having simultaneous measurement of those three fluids avoids the errors that can be introduced, due to the light fluctuations, when one optical channel is measured at a time.

The economic viability of on-chip microlaboratories depends on the possibility of implementing the detection and readout system in a standard microelectronic process (preferable CMOS). This means that the complete optical detection die would have to fit in an unaltered CMOS process, using only the layers available and without additional masks or process steps. This paper is concerned with this implementation: the detection die. It is an integrated CMOS chip that comprises the optical detectors and readout circuits. Its operation is based on topside illumination of the microplate cuvettes array. The impinging light transmitted through the twelve fluid cuvettes is measured by twelve photodetectors placed exactly underneath the microplate cuvettes array (Fig. 1), forming twelve optical channels. Therefore, each cuvette has its own photodetector underneath and its own readout circuit that converts the photodetectors analog signal into a digital one for further computer interfacing.

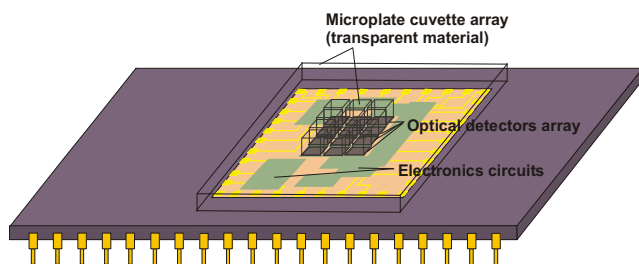


Fig. 1. Structure of the on-chip microlaboratory.

IV. SMART-OPTICAL DETECTOR ARRAY DESIGN AND SIMULATIONS

Fig. 2 shows the block diagram of the optical detector array. Each optical detector block comprises a photodetector and its own analog-to-digital (A/D) converter. The digital output signals of each column block are placed in separated output lines (Out1, Out2, etc.), while the output signals of each line block are placed in the same high-impedance output line (the four lines of Out1). This scheme is obtained addressing the lines array with clock signals shifted on time. Further computer processing perform additional calculations of these output signals to achieve a concentration value of the biochemical substance in analysis. Fig. 3 shows a detail of each block.

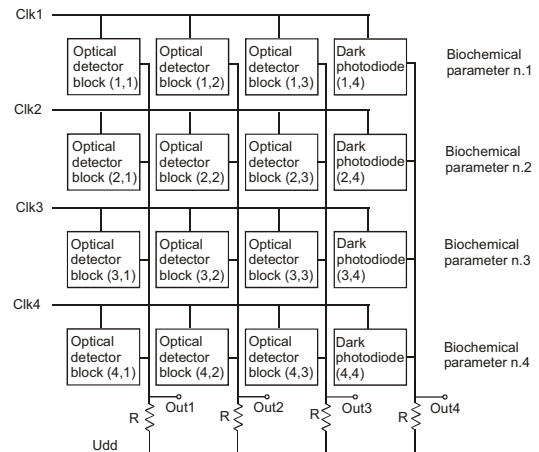


Fig. 2. Block diagram of the optical detector array.

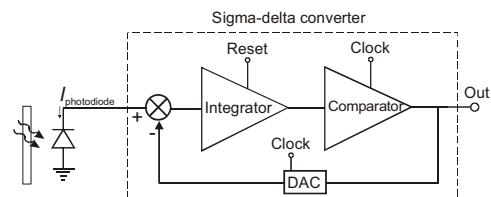


Fig. 3. Detection and readout circuit of each optical detector block.

A. Optical Detectors

The optical detectors convert the light intensity transmitted through the colored mixture into a photocurrent. Since CMOS technology rules must be met, the photodetectors are pn-junction photodiodes fabricated using the layers available in a CMOS standard process, without additional masks or steps. Basically, they use the junction between the $n+$ implant layer, used for drain and source contacts, and the p -epilayer [6]. An additional photodiode for measuring the photodiode dark current is introduced in the circuit. The dark current is the current that flows in a photodiode when there is no optical radiation incident on it. It is usually measured and subtracted to the further measurements. Since the dark current is temperature dependent, one measurement at the beginning of the experiment is usually not enough. Thus, in the reported circuit,

a dark current compensation channel is implemented. This photodiode is completely covered with metal.

B. Sigma-Delta A/D Converter

The on-chip A/D conversion is performed using a sigma-delta converter for each photodiode. The oversample frequency of the sigma-delta converters is determined by the desired number of output bits (signal-to-noise ratio). Therefore, the oversampling principle allows a flexible trade-off between bandwidth and accuracy (noise). In this concrete application, since the input signal has no time variations and since the bandwidth allowed by the CMOS circuits is much higher than the required bandwidth for the light measurement, a first-order one-bit sigma-delta converter with a high oversampling ratio and not a so high-clock frequency can be used.

From Fig. 3 it can be seen that the sigma-delta converter comprises three main blocks: the integrator, the comparator and the one-bit digital-to-analog converter (DAC). These blocks are described in detail in the following paragraphs.

The integrator is based in a current mirror (Fig. 4). The mosfet $M3$ is used to initialize the integrator with a known voltage level at the beginning of each conversion. This initialization allows an improvement of 3 dB in the signal-to-noise ratio of the sigma-delta converter [7].

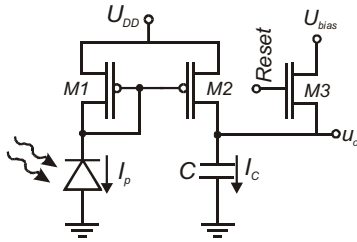


Fig. 4. Integrator based in a current mirror.

Once the gate-source voltages of $M1$ and $M2$ are the same, the photodiode current, I_p , is equal to the drain current of $M2$ if both mosfets are identical and if they are operating in the saturation region. The drain current of $M1$, I_{D1} , and of $M2$, I_{D2} , is given by (neglecting the channel-length modulation):

$$I_{D1} = I_p = \frac{1}{2}kp \frac{W_1}{L_1} (U_{GS1} - U_{thp})^2 \quad (2)$$

$$I_{D2} = I_C = \frac{1}{2}kp \frac{W_2}{L_2} (U_{GS2} - U_{thp})^2 \quad (3)$$

where kp is the transconductance parameter of the p-channel mosfet, W is the mosfet channel width, L is the mosfet channel length, U_{GS} is the gate-source voltage of the mosfet and U_{thp} is the threshold voltage of the p-channel mosfet. As $U_{GS1} = U_{GS2}$ (due to the diode connection of $M1$), the relationship between the two drain currents is:

$$\frac{I_{D1}}{I_{D2}} = \frac{W_2 / L_2}{W_1 / L_1} \quad (4)$$

This relationship shows that I_{D2} can be adjusted or amplified by changing only the mosfet widths and lengths. Moreover, as $I_{D2} = I_C$, this current charges the capacitor. Therefore, this circuit works as an integrator (with amplification if $I_{D2} > I_{D1}$).

The maximum integrator output voltage, U_O , is limited by the saturation region of $M2$:

$$U_{O,max} = U_{DD} - U_{Dsat} = U_{DD} - (U_{GS2} - U_{thp}) \quad (5)$$

The output resistance of the current mirror, r_o , is given by the output resistance of $M2$:

$$r_o = 1 / \lambda I_o \quad (6)$$

where λ is the channel-length modulation parameter.

The analysis of the integrator gain can be made with the help of its small-signal equivalent circuit (Fig. 5).

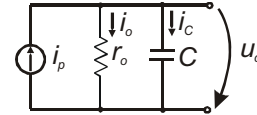


Fig. 5. Small-signal circuit model of the integrator.

In this circuit, $i_p = i_o + i_C$, $i_o = u_o / r_o$ and $i_C = C du_o / dt$. If $A = -1/r_o C$ and $B = 1/C$,

$$\frac{du_o}{dt} = Au_o + Bi_p \quad (7)$$

If the circuit is sampled with a sampling period, h :

$$u_o(h+1) = e^{Ah}u_o(h) + \frac{B}{A}(e^{Ah} - 1)i_p(h) \quad (8)$$

if,

$$e^{Ah} = S \quad \text{and} \quad \frac{B}{A}(e^{Ah} - 1) = T$$

The transfer function is given by:

$$H(z) = \frac{Tz^{-1}}{1 - Sz^{-1}} \quad (9)$$

and the DC gain is:

$$H(1) = -\frac{B}{A} = r_o \quad (10)$$

Equation 10 shows that the integrator gain is very high, so, it is finite and higher than the oversampling ratio. At these

conditions, the noise within the signal bandwidth only increases 0.3 dB [8].

Fig. 6 shows the simulated output voltage of the integrator for photocurrents of 4 nA and 60 nA. The graph shows clearly the effect of r_o in the output signal. However, even for the 60 nA curve, the fit can still be considered linear, once its Pearson coefficient is 0.9827.

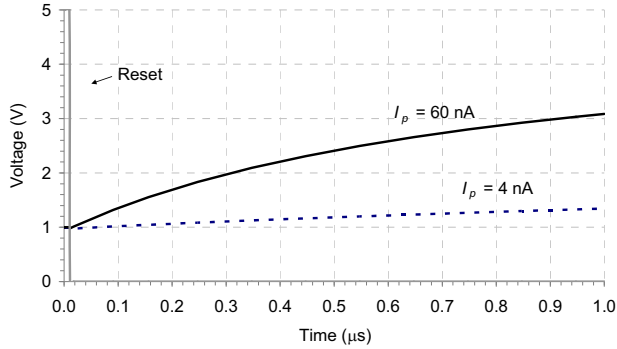


Fig. 6. Integrator output voltage during one clock period for photodiode currents of $I_p = 4$ nA and $I_p = 60$ nA.

Fig. 7 shows the schematic diagram of the comparator. Mosfets $M2$ and $M3$ form a differential pair that amplifies the voltage difference applied to their gates, U_{ref} and u_{in} , where U_{ref} is the input reference voltage of the comparator and u_{in} is the output voltage of the integrator. That difference is stored by $M5$ and $M6$, which work like a latch, in the fall down clock transitions, Clk . While the mosfet $M4$ is off (the clock signal is at low-level) the latch stores its state. The performance of the comparator is shown in Fig. 8 for a $U_{ref} = 2.5$ V and a randomly chosen input voltage, u_{in} . This figure shows that at each fall down clock transition, the output voltage of the comparator goes up if $u_{in} < U_{ref}$ and goes down if $u_{in} > U_{ref}$.

In this case, it is convenient to use a clock signal with a very low duty-cycle. There are two main reasons to do this: the first one is the fact that during the comparison (at the high-level clock), the input signal must be approximately constant; the second one will be explained during the description of the DAC converter.

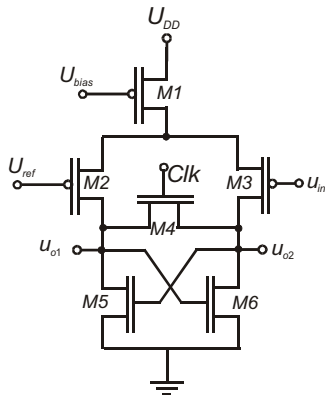


Fig. 7. Schematic diagram of the comparator.

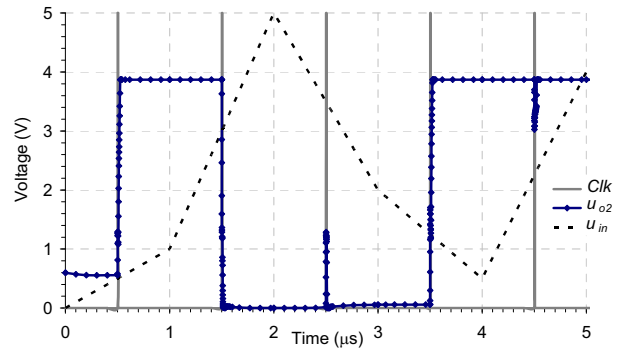


Fig. 8. Performance of the comparator.

The one-bit digital-to-analog converter is shown in Fig. 9. Ideally, the gain of the comparator should be infinite, it should perform an almost rail-to-rail output (u_{o2} between 0 V and U_{DD}). However, from Fig. 8 it can be seen that its output is not rail-to-rail. Therefore, it was integrated in the DAC circuit another comparator stage (performed by the mosfets $M1$ to $M6$), which allows increasing the global gain of the comparison (see Fig. 11). The mosfet $M8$ works as a voltage to current converter, e.g., it converts the digital output level into a current that will discharge the capacitor, C , of the integrator, whenever it is necessary and during the high-level of the clock signal (performed by $M7$). Once the clock signal has a small duty-cycle, the capacitor is discharged during a small time, allowing the use of small capacitance values, which is a suitable requirement for being integrated in CMOS.

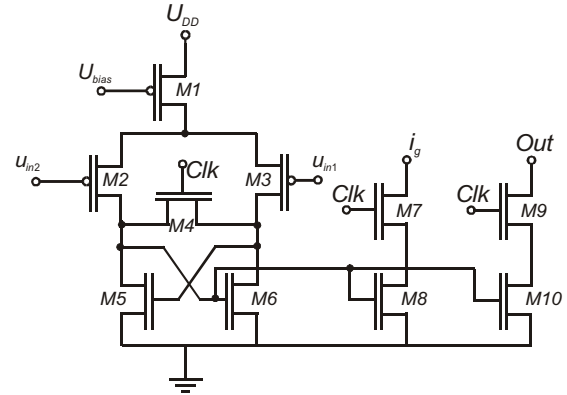


Fig. 9. One-bit digital-to-analog converter.

The performance of the sigma-delta converter working in closed loop can be seen in Fig. 10, for a $U_{ref} = 2.9$ V and a photodiode current of 10 nA. As the integrator output reaches 2.9 V (u_i), the comparator output voltage (u_o) goes up during one clock period. This voltage is converted to a current by the one-bit DAC converter that discharges the capacitor of the integrator. After this clock period, the capacitor starts its charging until the integrator output reaches 2.9 V, and the cycle will be repeated.

The output of each sigma-delta converter is obtained from this second stage comparator by the controlled current source formed by $M9$ and $M10$ (Fig. 9). This output is activated only in the high-level clock being in a high-impedance state at the low-level. This means that with small duty-cycles clock signals, the number of the detectors in the array can be increased if the clock signals that address the lines on the array are shifted on time. In addition, the detectors of the same column can share the same output wire. For instance, with a clock duty-cycle of 10%, the array can comprise 10 detectors sharing the same output wire, once each detector is read during a 10% of the clock period.

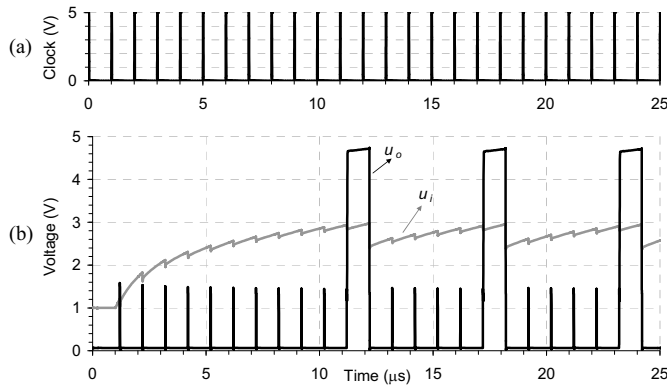


Fig. 10. Waveforms of the sigma-delta converter working in closed loop: (a) clock signal; (b) output voltage of the integrator (u_i) and of the comparator (u_o).

Fig. 11 shows the global circuit performance by the waveforms of the readout circuits of three optical detectors, placed in three different lines of the array (block (1,1), (2,1) and (3,1) according to Fig. 2). Each sigma-delta converter is addressed using clock signals shifted on time. The clock period is $1 \mu\text{s}$ with a 10 ns duty-cycle (it could be used a 100 lines array). The photodiodes currents are 4 nA (Fig. 10b), 60 nA (Fig. 10c) and 10 nA (Fig. 10d). From the detail of the output voltage of the first column for the three first lines array (Fig. 11f), it can be clearly seen when each sigma-delta converter is activated.

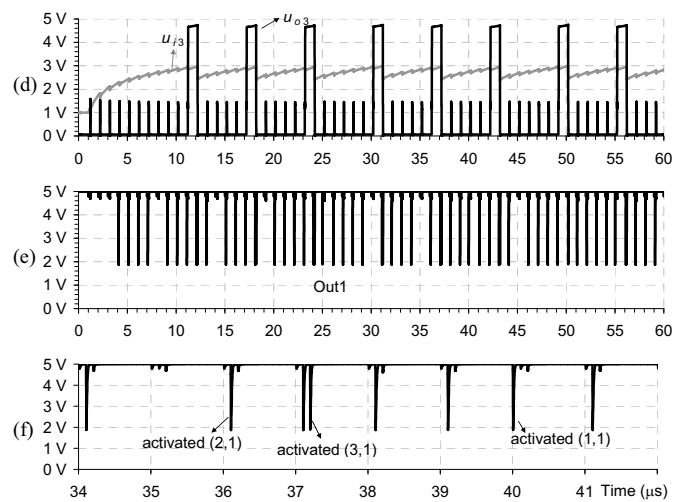
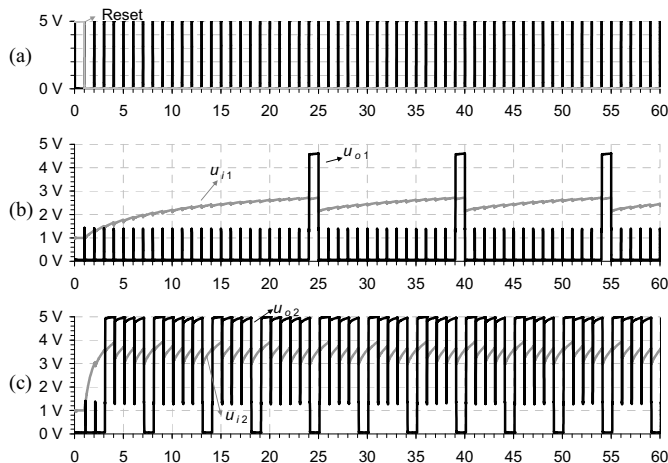


Fig. 11. Waveforms of three sigma-delta converters placed in different addressing lines of the array (see Fig. 2): (a) clock and reset signals; (b) integrator and comparator output voltage for converter (1,1); (c) integrator and comparator output voltage for converter (2,1); (d) integrator and comparator output voltage for converter (3,1); (e) output voltage Out1; (f) detail of the waveforms presented in (e).

V. SMART-OPTICAL DETECTOR ARRAY FABRICATION

Fig. 12 shows the complete microlaboratory. It consists on two dies. The first one is the microplate cuvette array for the physiological fluids. It is composed by twelve microfluidic cuvettes, which allows the analysis of four biochemical parameters simultaneous. It was fabricated using SU-8 techniques. The cuvettes have an area of $400 \mu\text{m} \times 400 \mu\text{m}$. The second die, placed underneath, is the detection chip. It has been fabricated through a $0.7 \mu\text{m}$ n-well CMOS process. It comprises the photodiodes (they have the same area as the cuvettes) and the corresponding A/D converters.

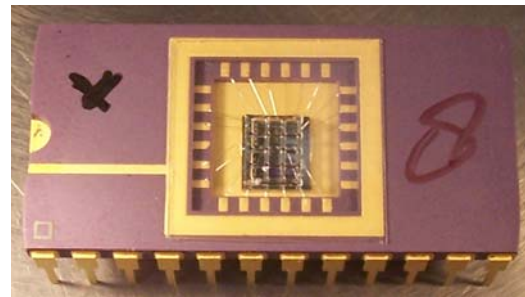


Fig. 12. Photograph of the complete microlaboratory. The microplate cuvettes array is glued on top of the detection chip.

Although the sigma-delta converters designed for this project have a very simple architecture, they have other advantages relatively to other interfacing devices used with the same purpose, namely, the noise that is integrated with the signal and then digitally filtered, which means that, except for its small quantity in the signal band, it is eliminated by the device. Moreover, they have small area which allows using one

converter for each photodetector allowing simultaneous measurements. This can be an advantage when it is necessary to relate the four biochemical parameters. Therefore, using this scheme they were measured at the same conditions.

VI. CONCLUSIONS

The CMOS integrated smart-optical detector array presented here enables the determination of biochemical parameters in physiological fluids. It has been developed to be an integrated part of an on-chip microlaboratory. The measurement is based on optical absorption in a well-defined part of the visible spectrum. This microsystem is composed by photodetectors each one with its A/D conversion for readout. The relatively simple readout circuits and the compliance with a standard CMOS process (without extra masks) allow addition of this smart-optical detection microsystem to an existing CMOS design. For the biochemical substance analysis, the microlaboratory operation requires the simultaneous measurement of the optical absorption of the fluid samples within several fluid cuvettes. Therefore, it was designed a first-order one-bit sigma-delta analog-to-digital converter for each optical channel (cuvette plus photodetector). The converter was designed with a small number of mosfets, occupying a very small area in the device. The simulation results have shown a promising performance, not only for this particular application, but for all applications where an array of photodetectors must be read. Meanwhile, the measurement and test setup are being

developed to obtain the so desired experimental results of the device.

ACKNOWLEDGMENT

Support for this research was provided by the Engineering School of University of Minho (program IN²TEC) and the R&D Centre Algoritmi of University of Minho.

REFERENCES

- [1] P. Connolly, "Clinical diagnostics opportunities for biosensors and bioelectronics," *Biosensors & Bioelectronics*, vol. 10, pp. 1-6, 1995.
- [2] A.J. Tudos, G.A.J. Besselink and R.B.M. Schasfoort, "Trends in miniaturized total analysis systems for point-of-care testing in clinical chemistry." *Lab Chip*, vol. 1, pp. 83-95, 2001.
- [3] S.C. Jakeway, A.J. de Mello and E. Russell, "Miniaturized total analysis systems for biological analysis," *Fresenius J. Anal. Chem.*, vol. 366, pp. 525-539, 2000.
- [4] *Biochemistry and Organic Reagents: for bioscience investigation*. Sigma-Aldrich Diagnostics®, 2002.
- [5] D.A. Skoog, D.M. West and F.J. Holler, *Fundamentals of analytical chemistry*. Saunders College Publishing, Orlando, Florida 1996, pp. 497-524.
- [6] G. Minas, J.C. Ribeiro, R.F. Wolfenbuttel and J.H. Correia, "On-chip integrated CMOS optical detection microsystem for spectrophotometric analysis in biological microfluidic systems," *In Proceedings of ISIE05*, Dubrovnik, Croatia, 20-23 June, pp. 1133-1138, 2005.
- [7] A.N. Netravali, Optimum digital filters for interpolative A/D converters, *Bell Syst. Tech. J.*, vol. 56, pp. 1629-1641, 1977.
- [8] J.C. Candy and G.C. Temes, editors, *Oversampled Delta-Sigma Data Converters*, IEEE Press, New York, 1992.